PHOTOOXIDATION OF WOOL DYE AND TCP IN AQUEOUS SOLUTION USING AN INOVATIVE TiO_2 MESH ELECTRODE

X. Z. Li, P. T. Yue and C. L. Mak*

Dept. of Civil and Structural Engineering, The Hong Kong Polytechnic University
**Dept. of Applied Physics, The Hong Kong Polytechnic University*
Hung Hom, Kowloon, Hong Kong

ABSTRACT

An innovative titanium dioxide (TiO_2) mesh electrode was prepared by anodisation, in which 0.5M sulphuric acid was used as electrolyte and titanium (Ti) metal mash was anodised in a two-stage anodic process. The innovated mesh electrode was examined using Raman spectroscopy to determine the formation of TiO_2 layer when different potential of 120V, 140V, 160V and 180V were applied in anodisation. Microporous surface of the electrode was also examined using scanning electron microscopy. The photocatalytic (PC) oxidation and photoelectrocatalytic (PEC) oxidation were studied using the new electrode for treating synthetic wastewater solutions of dye and trichlorophenol (TCP) respectively. The colour removal efficiency of 68% was achieved using the 160V-mesh electrode for treating wool dye solution after 80minutes reaction time. However, It was found that a significant substrate adsorption on the surface of the mesh electrode could not be avoided when pH was below pH_{IEP} of TiO_2 = 6.3. In this condition, electrostatic adsorption occurred between the anionic substrate molecules and positively charged TiO_2 surface. The adsorbed substrate anion occupied most active sites of TiO_2 on the mesh

electrode surface and significantly reduced the performance efficiency of photo-oxidation, when the TiO_2 mesh electrode was reused. The experiment demonstrated that TCP adsorption on the mesh electrode could be significantly eliminated, when pH of TCP solution was adjusted to above 7. When raising pH in TCP photodegradation eliminated substrate adsorption, it was confirmed that PC oxidation with applying a potential bias could enhance the photo-oxidation rate and a repeatable photo-oxidation rate could be maintained when same mesh electrode was reused in its following tests.

KEYWORDS:

Anodic oxidation; titanium dioxide; photoelectrocatalytic oxidation; wool dye; trichlorophenol.

INTRODUCTION

Since Carey et al. in 1976 carried out the first study that UV irradiation of aqueous suspension of TiO_2 containing polychlorinated biphenyls (PCBs), the feasibility of the photo-oxidation reaction to completely oxidise almost organic compounds dissolved in water at laboratory scale experiment has been extensively demonstrated in the past two decades (Aurian-Blajeni and Halmann, 1980; Nguyen and Ollis 1984; Augugliaro, 1988; Mathews, 1993; Chen and Ray, 1998). Organic dyes are one of the complex organic compounds. Several researchers have reported the photocatalytic oxidation of dyeing wastewater, that included Methyl violet (Tennakone et al., 1989); Azo dyes (Hustert and Zepp, 1992); methylene blue (S. Lakshmi et al., 1995) and Rhodamine B (Ma and Yao, 1998).

To conduct the heterogeneous photocatalysis with semiconductors such as TiO_2, either the photocatalyst may disperse in suspension, or it may be coated on the rigid body of reactant chamber (Aurian-Blajeni and Halmann, 1980). The degradation rate of *p*-toluenesulphonic acid (PTSA) by immobilised TiO_2 photocatalyst was lower than suspended TiO_2 particles (Brezova et al., 1994). Though the photodegradation of organic pollutants in TiO_2 suspension is very effective, it is difficult to separate and recover the photocatalyst such as by filtration. (Zhao and Hidaka, 1993). In a suspension system, another concerned problem is that TiO_2 particles behave as shortcircuited microelectrodes under bandgap excitation. High degree of recombination between photogenerated charge carriers wastes radiation energy. Therefore, electrochemically assisted photocatalytic oxidation was introduced to improve the oxidation activity and eliminate the TiO_2 recovery process. Vindogopal et al. (1993) successfully proved that the photocatalytic oxidation efficiency can be enhanced by applying an anodic bias to a TiO_2 particulate film electrode on conducting glass plate to degrade 4-chlorophenol, whiles the platinum rod acts as counter electrode. It is because the photogenerated electrons on TiO_2 was driven away to prevent charges recombination. Later, several studies for degrading formic acid, amino acids and 4-chlorocatechol was conducted by other researchers (Kim and Anderson, 1994; Hidaka et al. 1997; Kesselman, 1997). However, in their studies, the photo-anode was only prepared by coating TiO_2 on conducting glass that covered by an indium tin-oxide. Mass transfer of reactants on the immobilised flat surface was quite low.

In this study, an innovative photo-anode was prepared by an anodic oxidation process. Raman spectroscopy and Scanning Electron Microscope (SEM) were used to examine the mineral formation and morphology of the oxide layer respectively. The photo-oxidation efficiency of the innovated mesh electrode was also studied in the treatment of synthetic wool dye solution and TCP solution.

EXPERIMENTAL METHODS

Anodisation process: Commercially pure (>99%) titanium mesh was purchased from Goodfellow Cambridge Limited. The weave pattern of mesh is twill. Nominal aperture and wire diameter are 0.19 mm and 0.23 mm respectively, whiles open area percentage is 20%. 30 mm x 10 mm of anode was cut off from a large mesh without further purification. The counterelectrode used in the anodic oxidation process was a copper plate with similar size and 0.5M sulphuric acid with analytical grade was prepared and used as electrolyte. A laboratory-made DC power supply was used to provide required potential and current in the experiment. Anodisation process was conducted in two stages, in which galvanostatic anodisation was first performed until a designed anode-to-cathode voltage (120V, 140V, 160V and 180V) was reached with a constant current density of 110 mA/cm^2. Then the constant voltage was maintained until the end of anodisation, while the current was gradually decreasing. The whole process of anodisation lasted for 10 minutes in all the tests. The freshly generated TiO_2 mesh electrode was then rinsed by distilled water and dried in an oven at 105^oC for half an hour.

PC/PEC oxidation reactor: The photo-reactor used in the experiment was a quartz cell with the size of 25 mm in diameter and 50 mm in length. An 8W-actinic lamp was used as the light source with a maximum emission peak of 365 nm. All photoreaction tests were carried out in the reactor and about 10 ml of synthetic aqueous solution was used in each test. The distance between the lamp and the reactor was 5 mm and a light intensity of $2.8x10^3$ $\mu W/cm^2$ on the anodic TiO_2 mesh electrode was measured by a Blak-Ray UV meter (UVP Inc, Model No. J221). A potentiostat (ISO-TECH 1PS 1810H) was used to provide an anodic bias to the photo-anode, while the cathode was a Cu wire (40 mm in length and 2mm in diameter). Air was supplied to the system through a glass air diffuser, which also provided turbulence in the solution.

Synthetic wastewater: Synthetic dye solution was prepared by well dissolving the dye powder (Polar yellow GN-01 400%) from Ciba Speciality Chemicals Limited in distilled water. The dye stock solution of 400 mg/L was prepared first and was diluted to 50 mg/L prior to the tests. 2,4,6-Trichlorophenol (TCP) obtained from Riedel-dehaen (cat.no.63127, 97%) was used without further purification. The TCP stock solution of 100 mg/L was prepared with distilled water first and diluted to the desired concentration prior to the tests.

ANALYTICAL METHODS

Structural analysis: Raman spectroscopy was used to determine the formation of TiO_2 (anatase and rutile) on the mesh electrode. The room temperature Raman spectra were excited by 514.5nm laser line from a CW argon laser (Coherent Innva 70). The laser power was kept at 250 mW to avoid laser annealing of the samples. A 55mm f/1.8 lens was used for collecting the scattering light which was dispersed and detected using a double grating monochromator (Spex 1403) equipped with a cooled photomultiplier tube (PMT, Hamamatus R943-2). All spectra were recorded in the small angle scattering geometry. The resolution obtained was expected to be as good as 1 cm^{-1}.

Surface analysis: Scanning Electron Microscopy (Leica Stereoscan 400i Series) was used to study the surface

morphology, average pore size and pores distribution. High tension was selected at 15kV.

Decolorisation analysis: The colour removal of the dye sample was determined by measuring the absorption spectra of solution. An auto-scan spectrophotometer (Genesys 2 – Milton Roy) was used with a wavelength range of 300-550 nm. 2-ml solution sample was taken from the reactor for measurement and was put back to the reactor after each measurement.

TCP analysis: TCP in solution was analysed by a High Performance Liquid Chromatography (HPLC), which comprised a ISCO, Model 2350 pump and a UV detector (Waters^{TM} 486, Turnable absorbance detector) at 289 nm wavelength. A reverse-phase column (Symmetry C18) was used with 150 mm in length and 3.9 mm in diameter. The mobile phase was a mixture of acetonitrile (47%), demonised distilled water (52%) and acetic acid (1%).

RESULTS AND DISCUSSION

Two-stage anodisation process

In most anodic oxidation process, metals can dissolute in aqueous acidic solution under enough potential bias or current in the process to form an oxide layer on the metal surface. In this study, the formation of TiO_2 was conducted on a piece of Ti-metal mesh. 0.5M sulphuric acid was used as electrolyte due to its low cost and ease of preparation. In this two-stage mode, the galvanostatic anodisation was applied first and characterised by a fast increase of the potential difference across the oxide layer at the beginning of the process (i.e. 1.2V/s). This increase then slowed due to the effective activation energy of oxide growth reached a near constant level. At this point, the dissolution rate equals to the oxidation rate. Theoretically, higher anodic growth rate is given by a higher current density or activation energy on the electrode. Also, electric field around the electrode is also directly proportional to the current density. In the second stage, after the voltage reached the designed maximum value, a constant voltage (120V, 140V, 160V and 180V) was maintained, while the current intensity was decreasing.

The variation of voltage and current density against time in the anodisation process is shown in Figure 1. A linear relationship between voltage and time was obtained during the initial 1.25 minutes in all the cases while a constant current density was maintained. The anodic growth rate can be obtained from the curve to be 1.2V/s (up to 1.25minutes), when the current density was 110 mA/cm^2. However, the slope of voltage curve was getting more flat owing to limited power given from the DC power supply. The current across the electrodes dropped rapidly since the resistance increased. It was observed that fine gas bubbles were generated from both anode (Ti-mesh) and cathode (Cu-plate), and even gas film could be seen on the surface of the solution. The generation rate of the gas on the cathode was greater than that on the anode. It was because most of the oxygen molecules generated at the anode were combined with Titanium to form the titanium oxide, whiles hydrogen gas generated at the cathode was liberated freely.

Raman spectroscopy

Both the raw Ti-mesh and the TiO_2-mesh electrodes prepared using different voltage were examined by ex-situ

Raman spectroscopy. Their Raman spectra are shown in Figure 2, in which the peaks representing the anatase and rutile forms of TiO_2 are labelled with A and R respectively. The phonon peaks of anatase were located at 147, 200, 393, 516 and 640 cm^{-1}, whiles the phonon peaks of rutile were observed at 244, 445 and 612 cm^{-1}. The strongest peak of anatase occurred at around 147 cm^{-1} with a narrow line shape in all the cases, while other peaks were broader. Up to 140V, the Raman spectra showed that the main anatase peaks were increasing while the applied voltage increased. Above 160V, additional peaks corresponding to the rutile phase of TiO_2 were

developed. The spectra also indicate that the anatase phase of TiO_2 was dominant in all the cases with a voltage

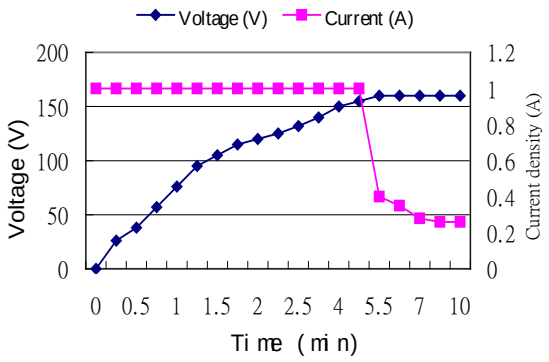

Figure 1. Two-stage anodic oxidation process

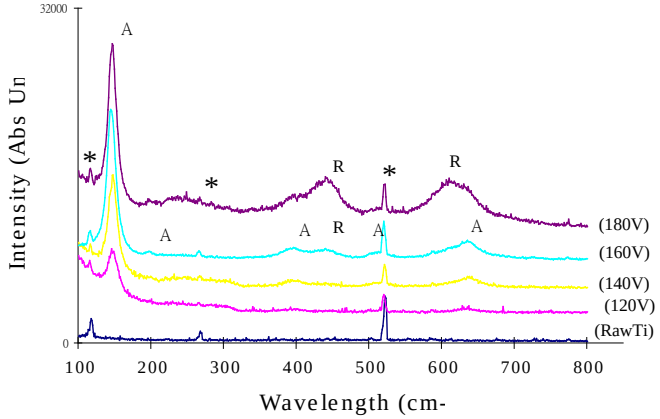

Figure 2. Raman spectrum of Ti and TiO_2 mesh

growth rate of 1.2V/s.

Scanning Electron Microscope (SEM)

By eyes observation, the raw Ti-mesh was in silver colour, the TiO_2-mesh electrode prepared at 120V was in sky blue, the TiO_2-mesh electrode prepared at 140V was in light grey with blue, the TiO_2-mesh electrode prepared at 160V was in light grey and the TiO_2-mesh electrode prepared at 180V was in grey. When anodising titanium, the sparking breakdown voltage that could be achieved was 130V in 0.5M sulphuric acid under galvanostatic mode anodisation, in which the colour of the oxide layer was changed to grey and the surface reflectivity decreases rapidly. The different colour obtained in oxidised films below the sparking voltage was due to light interference.

Mikula et al. (1992) concluded that when anodising current density is greater than 30 mA/cm^2 in sulphuric acid, the power dissipated in the barrier oxide layer increases considerably. It causes the overheating of local oxide, and the cooling of the oxidised anode by the electrolyte becomes insufficient. This higher temperature leads to a higher ionic current probably along grain boundaries, and the oxide may recrystallise and results in a porous surface. When the current densities greater than 100 mA/cm^2, a fast dissolution of the oxide is believed to occur with the creation of pores. Which lead to an even rougher surface. In this experiment, since a constant current density was applied in the first stage, the diameter of the pore size increased with potential raise during anodisation and was measured directly from the SEM micrograph. The SEM results show that while a higher voltage applied to the anodisation process, more power dissipation was expected in the oxide layer to finally form the micropore of TiO_2 surface with a larger size. When the voltage was applied from 120 – 180 V, the micropore size increased from 17 to 60 nm. Three SEM micrographs of the raw Ti-mesh surface and the TiO_2-mesh electrodes prepared at 120V and 180V are shown in Figure 3 respectively.

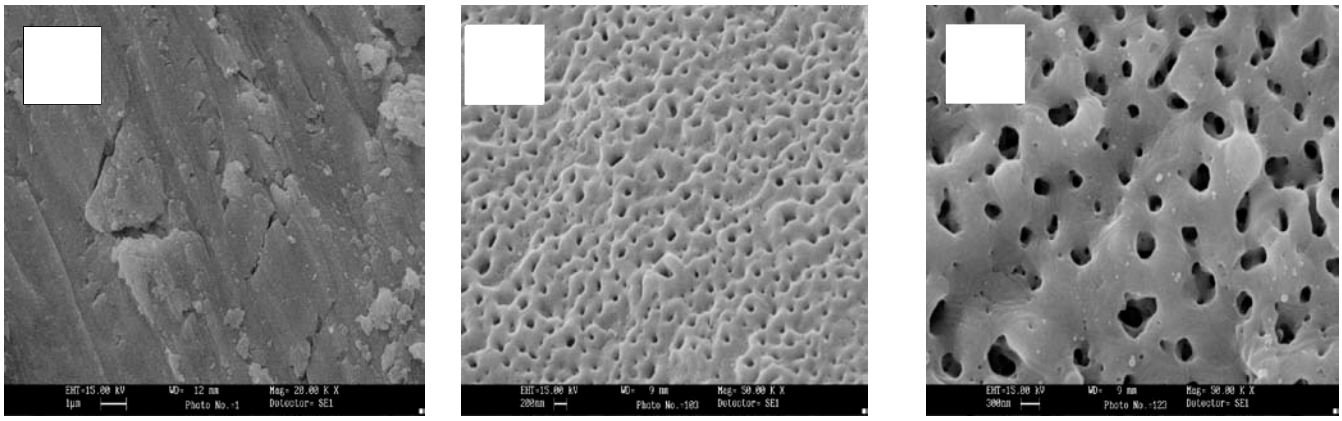

Figure 3. SEM micrographs of A-raw Ti-mesh, B-120V TiO_2-mesh and C-180V TiO_2-mesh

Decolorisation of dyeing solution

Two TiO_2-mesh electrodes prepared at 140V and 160V were used in this experiment to conduct the photocatalytic (PC) oxidation and photoelectrocatalytic (PEC) oxidation as they contained a higher portion of anatase forms in the structure based on the Raman spectrum results. 50 mg/L wool dye (Polar yellow GN-01 400%) solution was photo-oxidised in the designed photoreactor, in which fine air bubbles were released from an air diffuser and provided a turbulent flow with saturated oxygen to facilitate the photocatalytic oxidation. The absorption spectrum of the dye solution was monitored during the photocatalytic oxidation as shown in Figure 4. After 80 minutes reaction time, colour removal of the dyeing solution was achieved to 68%. A blank test without TiO_2 electrode was also conducted to confirm no direct photolysis oxidation from the UV source. After the first

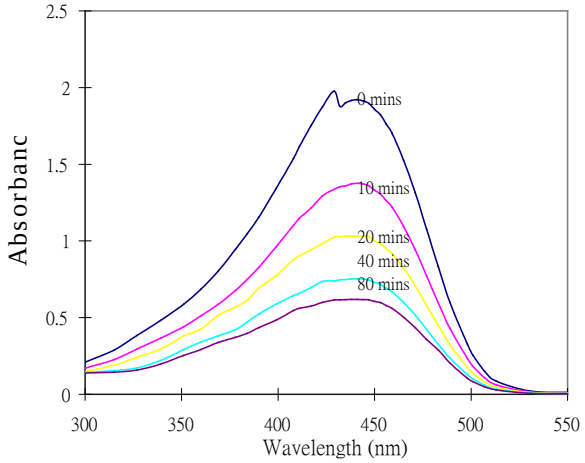

Figure 4. Absorption spectrum of wool dye solution in PE oxidation

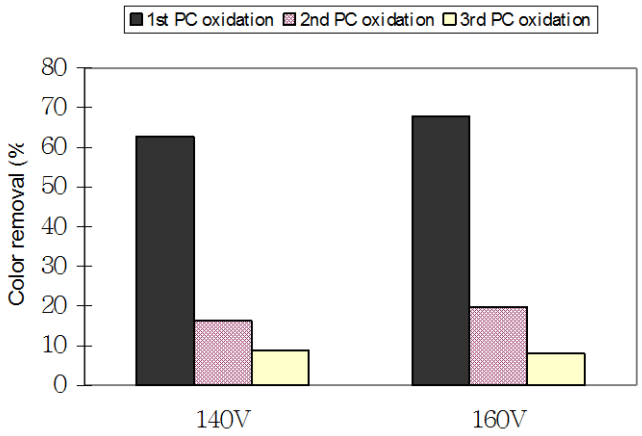

Figure 5. Colour removal of wool dye solution in PE oxidation

photocatalytic oxidation test, both TiO_2-mesh electrodes were rinsed with distilled water and reused for the following photocatalytic oxidation again. However, it was found that the colour removal efficiency in the following tests with same electrode was dramatically decreased as shown in Figure 5.

The experiment demonstrated that the TiO_2 surface of the electrode became much less active after the first test. To determine the reason causing efficiency lost, another test was conducted in a dark condition without UV irradiation and the results as shown in Figure 6 indicate that the wool dye residual in solution can be strongly adsorbed by the microporous surface of TiO_2 layer on the mesh electrode. About 36% colour removal was achieved due to the absorption by 140V electrode, while about 25% by 160V electrode. Once the TiO_2 surface was covered by the adsorbed dye residual, the effective surface of TiO_2 for photocatalytic oxidation was greatly reduced.

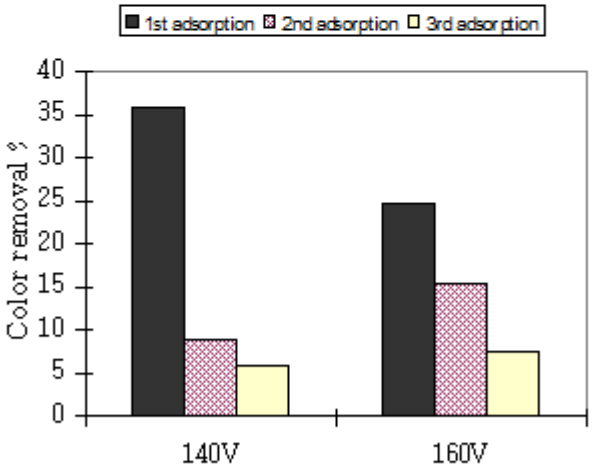

Figure 6. Colour removal by adsorption only

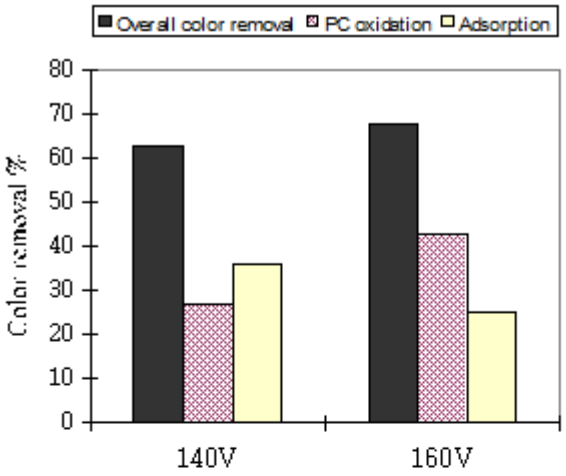

Figure 7. Distribution of colour removal

After three tests, the dye residual has covered most surface area of the electrode, which resulted in the decrease of photo-oxidation efficiency. Based on the results shown in Figure 5 and 6, a distribution of colour removal due to adsorption and photo-oxidation can be figured out as shown in Figure 7. This study indicates that once adsorption exists, the overall colour reduction will be resulted by both photo-oxidation and also adsorption.

Degradation of TCP in aqueous solution

To eliminate the substrate adsorption on the electrode, control of pH is an important option. Since the pH of the dyeing wastewater sample in the experiment was 5.7 and can be characterised as an ionic dye. The TiO_2 surface is composed of amphoteric sites, which can become charged either positively or negatively depending on the solution pH while the isoelectric point of TiO_2 (pH_{IEP}) is 6.3 (Shuzo et al. 1994). In aqueous solution the surface of TiO_2 is covered with hydroxyl groups as well as molecular water and is negatively charged at pH>6.3, whiles positively charged at pH<6.3. Therefore, electrostatic absorption would occur in both PC oxidation and PEC oxidation, if the experiment is conducted in the condition of pH=5.7. Specially in PEC oxidation, since the electron generated on TiO_2 surface is driven away in photo-oxidation, the positive charge carriers (holes) remain

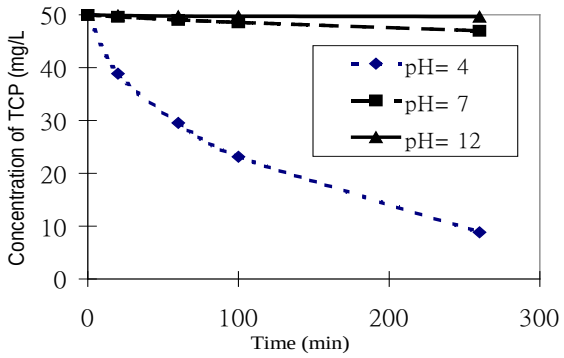

on the oxide surface to make it more positive and a higher adsorption rate can be expected due to a higher electrostatic force between the opposite charged ionic substrate and oxide surface.

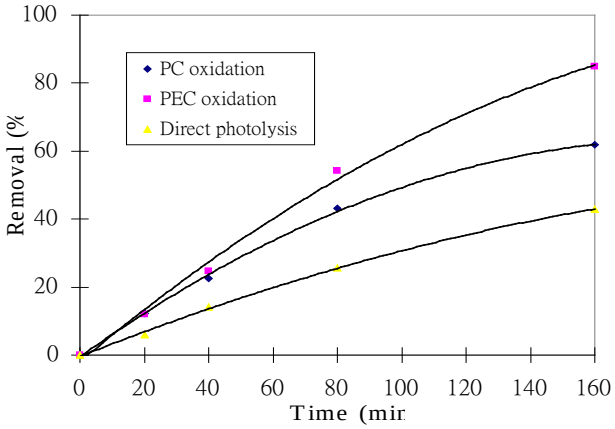

Figure 8. Absorption of 2,4,6 TCP on TiO_2 mesh electrode at pH=4, 7, 12.

Figure 9. Photodegradation of TCP at pH=12 by Photolysis, PE oxidation and PEC oxidation

The pH effect was considered in this experiment. 50-mg/L TCP solution with different initial pH of 4,7 and12 were first treated in a dark condition to study the adsorption characters. These 3 tests were conducted for 260 minutes respectively and the TCP adsorption by the mesh electrode is shown in Figure 8. The results indicate that a strong TCP adsorption (>80%) on the electrode occurred in the condition of pH=4 and a much weaker adsorption (<10%) was found in the condition of pH=7, while nearly no TCP adsorption occurred in the condition of pH=12. It may indicate that when TCP becomes the negatively changed trichlorophenoxide at a higher pH condition, the repulsion between the negatively charged TiO_2 surface and tichlorophenoxide can inhibit their adsorption.

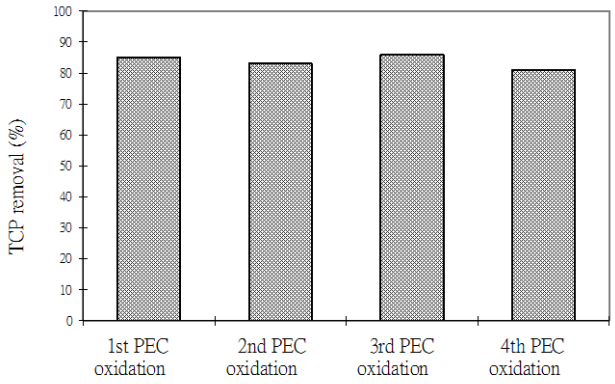

Figure 10. PEC oxidation efficiencie tests using same 160V TiO2 electrc

To study the performance of PEC and PC oxidation without adsorption interference, 20-mg/L TCP solution with initial pH=12 was photo-oxidised in the same reactor. Three tests were respectively conducted by UV radiation only, PE oxidation and PEC oxidation with an potential bias of +0.6V. The experimental results as shown in Figure 9 demonstrate that degradation of TCP in its aqueous solution was achieved to 61% and 85% after 160min reaction for PC and PEC oxidation respectively,

while only 43% TCP was degraded by pure photolysis under UV radiation. These results confirmed that the PEC oxidation can enhance the PC oxidation efficiency, since electrons can be driven away and the holes remain on TiO_2 surface to form hydroxyl radical. It may be also implied that more rapid oxidation can eliminate the substrate adsorption in this photo-oxidation.

To test the repeatability of photo-oxidation efficiency of TiO_2-mesh electrode, 4 PEC oxidation tests were continued using the same electrode repeatedly. After each test, the TiO_2-mesh electrode was only washed by distilled water and dried using a blower. The experimental results are shown in Figure 10, which demonstrate a constant efficiency of PEC oxidation in the range of 80 – 85%.

CONCLUSIONS

A TiO_2 layer was successfully formed on Ti-metal mesh by anodic oxidation in 0.5M sulphuric acid. Anatase mineral form was found to be dominant in the TiO_2 layer, when an anodic growth rate of 1.2V/s was applied. Rough microporous surface of the TiO_2-mesh electrode in the dyeing solution with a low pH (pH<6) caused a significant substrate adsorption. The adsorbed substrate anion occupied most active sites of TiO_2 on the mesh electrode surface and significantly reduced the performance efficiency of photo-oxidation, when the electrode was reused. The experiment of TCP degradation demonstrated that the TCP adsorbed on the mesh electrode could be significantly eliminated, when the pH of TCP solution was adjusted to above 7. When raising pH in TCP photodegradation eliminated substrate adsorption, it was confirmed that PC oxidation applying a potential bias as

PEC oxidation could enhance the photo-oxidation rate. When TCP solution was photo-oxidised at a high pH, similar photo-oxidation rate could be maintained when the same mesh electrode was reused.

REFERENCES

Arsov L.D., Kormann C. and Plieth W. (1991). In situ raman sepectra of anodically formed titanium dioxide layers in solution of H_2SO_4, KOH, and HNO_3, *J. Electrochem. Soc*, **138**(10), 2964-2970

Augugliaro, V. (1988). Photocatalytic degradation of phenol in aqueous titanium dispersion, *Toxicol. Environ. Chem*., **16**, 89-109.

Aurian-Blajeni, B and Halmann, M. (1980). Photoreduction of Carbon Dioxide and Water into Formaldehyde and Methanol on Semiconductor Materials, *Solar Energy*, **25**, 165-170.

Brezova, V., Jankovicova, M., Soldan, M., Blazkova, A., Rehakova, M., Surina, I., Ceppan, M. and Havlinova, B. (1994). Photocatalytic degradation of p-touenesulphonic acid in aqueous systems containing powdered and immobilised titanium dioxide, *Journal of Photochemistry and Photobiology A: Chemistry*, **83**, 69-75.

Carey, J. H. (1976). Photodechlorination of PCBs in the Presence of Titanium Dioxide in Aqueous Suspensions, *Bull. Environ. Contam. Toxiol*., **16**(6), 663-677.

Chen, D.W. and Ray, A.K. (1998). Photodegradation kinetics of 4-nitrophenol in TiO_2 suspension, *Water Research*, **32**(11), 3223-3234.

Hidaka H., Kazuhiko, T. S., Zhao J. and Serpone, N., (1997). Photoelectrochemical decomposition of amino acids on a TiO_2/OTE particulate film electrode, *Journal of Photochemistry and Photobiology A: Chemistry*, **109**, 165-170.

Hustert, K. and Zepp, R.G. (1992). Photocatalytic degradation of selected azo dyes, *Chemosphere*, **24**, 335-342.

Kesselman, J. M., Lewis, N. S. and Hoffmann, M. R. (1997). Photoelectrochemical degradation of 4-chlorocatechl at TiO_2 electrodes: Comparison between sorption and photoreactivity, *Environ. Sci. Technol*, **31**, 2298-2302.

Kim, D. H. and Anderson, M. A. (1994). Photoelectrolytic Degradation of Formic Acid Using a Porous TiO_2 Thin-Film Electrode, *Environ. Sci. Technol*., **28**, 479-483.

Lakshmi, S., Renganathan, R., and Fujita, S. (1995). Study on TiO_2-mediated photocatalytic degradation of methylene blue, *Journal of Photochemistry and Photobiology A: Chemistry*, **88**, 163-167.

Ma, Y. and Yao, J. N. (1998). Photodegradation of Rhodamine B catalyzed by TiO_2 thin film, *Journal of Photochemistry and Photobiology A: Chemistry*, **116**, 167-170.

Matthews, R.W. (1993). Photo-oxidation of Organic Material in Aqueous Suspensions of Titanium Dioxide, *Wat. Res*, **24**(5), 635-660.

Mikula M., Blecha J. and Ceppan M. (1992). Photoelectrochemical properties of anoidic TiO_2 layers prepared by various current densities, *The electrochemical Society*, **9**(12), 3470-3474.

Nguyen, T. and Ollis, D.F. (1984). Omplete heterogeneously photocatalysed transformation of 1,1- and 1,2-dibromomethane to CO_2 and HBr, *J. Phys. Chem*., **88**, 3386-3388.

O' Shea, K. E. and Cardona, C. (1995). The reactivity of phenol in irradiated aqueous suspensions of TiO2 mechanistic changes as a function of solution pH, *Journal of Photochemistry and Photobiology A:*

Chemistry, **91**, 67-72.

Tanaka, S. and Saha, U. K. (1994). Effects of pH on photocatalysis of 2,4,6-trichlorophenol in aqueous TiO_2 suspensions, *Wat. Sci. Technol.*, **30**(9), 47-57

Tennakone, K., Punchiheva, S., Wickremanayaka, S. and Tantrigoda, R.U. (1989). Titanium dioxide catalysed photo-oxidation of methyl violet, *Journal of Photochemistry and Photobiology A: Chemistry*, **46**, 247-252.

Vinodgopal, K., Hotchandani, S. and Kamat, P. V. (1993). Electrochemically assisted photocatalysis. TiO2 particulate film electrodes for photocatalytic degradation of 4-chlorophenol, *J. Phys. Chem*, **97**, 9040-9044.

Zhao, J. and Hidaka, H. (1993). Photodegradation of Surfactants - Potential Measurements in the Photocatalytic Oxidation of Surfactants in Aqueous TiO_2 Dispersions, *Langmuir*, **9**, 1646-1650.